Image-Plate Synchrotron Laue Data Collection and Subsequent Structural Analysis of a Small Test Crystal of a Nickel-Containing Aluminophosphate

E. Snell,[a] J. Habash,[a] M. Helliwell,[a] J. R. Helliwell,[a]* J. Raftery,[a] V. Kaucic[b] and J. W. Campbell[c]

[a]*Department of Chemistry, University of Manchester, Manchester M13 9PL, UK,* [b]*National Institute of Chemistry and University of Ljubljana, 61000 Ljubljana, Slovenia, and* [c]*DRAL, Daresbury Laboratory, Warrington WA4 4AD, UK*

Image plates have advantages over photographic films, which include wider dynamic range, higher detector quantum efficiency, reduced exposure time and large size. In this study, an on-line image-plate system has been used to record crystallographic data from a small crystal. In particular, synchrotron Laue data were recorded with $\lambda_{min} = 0.455$, $\lambda_{max} = 1.180$ Å, in 20 images 10° apart and with an exposure time of 0.3 s each from a crystal ($0.02 \times 0.05 \times 0.25$ mm) of a nickel-containing aluminophosphate, NiAPO. The Laue data were analyzed with the Daresbury Laue software, including the application of an absorption correction. The structure was solved by a combination of the Patterson method and successive difference Fourier calculations using *SHELXS*86 and *SHELXL*93; the final R value for 1934 unique reflections (all data) and 310 parameters was 7.90%. The structure agrees with that determined by monochromatic diffractometry using the same crystal and reported by Helliwell, Gallois, Kariuki, Kaucic & Helliwell [*Acta Cryst.* (1993), **B49**, 420–428] with an r.m.s. deviation of 0.03 Å. Hence, this study shows the image-plate device to be very effective for synchrotron data collection and subsequent structure analysis from small crystals, *i.e.* $0.02 \times 0.05 \times 0.25$ mm, in chemical crystallography as well as providing further confirmation of the practicability of Laue data in structure solution and refinement.

Keywords: image plates; area detectors; synchrotron Laue method; pixel sampling.

1. Introduction

Image plates have had an important impact on X-ray crystallographic data collection from macromolecules, both at the synchrotron and in the home laboratory. Also, the advantageous speed of acquisition of area-detector data in chemical crystallography, compared with diffractometry, can be critical. For example, the number of reflections to be measured may be very large (*e.g.* 20 000 reflections), whether due to a larger than average unit cell, a low symmetry space group or an interest in very high resolution (*e.g.* 0.6 Å or better). Alternatively, a sample might be air sensitive and again speed of data collection may be critical.

At the synchrotron there is tremendous potential for data collection (*a*) from very small crystals (see, for example, Andrews, Papiz, McMeeking, Blake, Lowe, Franklin, Helliwell & Harding, 1988; Harding, 1990, 1991; Riekel, 1993; Bilderback, Thiel, Pahl & Brister, 1994), (*b*) involving the use of tunable wavelengths for anomalous-dispersion applications (Helliwell, Gallois, Kariuki, Kaucic & Helliwell, 1993) or (*c*) for perturbation studies. All these topics are reviewed by Coppens (1992).

The ease of data collection at the synchrotron, especially on time factors, can benefit from the use of a large versatile area detector like the image plate. Although photographic film has been used effectively in a number of synchrotron Laue studies of small molecules (*e.g.* Clucas, Harding & Maginn, 1988; Helliwell, Gomez de Anderez, Habash, Helliwell & Vernon, 1989; Harding, 1991), the use of film with smaller crystals is ultimately beset by the problem of very small or very narrow (streaked) spots for which the pixel sampling of the spot is too poor and/or the Wooster effect is a limitation. One aspect of this paper is to show that on-line image plates can readily be used with a small crystal to rapidly collect data with good pixel sampling of diffraction spots for structure determination and refinement. As a test case we have used the crystal structure of a nickel-containing aluminophosphate. This structure has been determined and reported recently using Cu $K\alpha$ and Mo $K\alpha$ diffractometry (Helliwell *et al.*, 1993). Attention has also been drawn to the use of image plates by Euler, Gilles & Will (1994), who reported on a synchrotron Laue study of olivine. Their initial impetus was clearly the same as our own. Our aim in this paper is the study of much smaller crystals than the 410 μm diameter olivine

---

* To whom correspondence should be addressed.

crystal case. Moreover, we go on to provide a full structural analysis. This paper, therefore, nicely complements that of Euler *et al.* (1994).

In the work of Andrews *et al.* (1988) with a very small, mosaic crystal of piperazine silicate, the Enraf–Nonius FAST television area-detector diffractometer was used with intense monochromatic synchrotron radiation. This detector is also an on-line system. Compared with the image plate it had fewer pixels and poorer resolution, but a faster duty cycle. A next generation of on-line detector beckons, combining a large aperture with fast duty cycle based on an array of CCDs (for a discussion, see Allinson, 1993) and without the need for an image intensifier (reviewed by Allinson, 1994).

For anomalous-dispersion studies, a particular wavelength is needed (*e.g.* Ni K edge 1.488 Å) and so the need for $d_{min} \leq 0.9$ Å in chemical crystallography implies $2\theta_{max}$ values of $\gtrsim 110°$ occur. Even longer wavelength absorption edges exacerbate this and a cylindrical geometry, *e.g.* realizing $2\theta_{max} = 180°$, is desired. Image plates can certainly be used in this geometry. An on-line cylindrical image-plate and reader design is described by Wilkinson (1994). Alternatively, the array concept of CCDs can be extended.

2. Experimental

A small needle-shaped crystal ($0.02 \times 0.05 \times 0.25$ mm) of NiAPO [NiAl$_3$P$_4$O$_{18}$C$_4$H$_{21}$N$_4$, $M_r = 676.77$, monoclinic, $P2_1/n$, $a = 10.02$, $b = 15.728$ (6), $c = 14.134$ (6) Å, $\beta = 101.313$ (14)°, $V = 2184.16$ Å^3, $Z = 4$, $D_x = 2.06$ g cm^{-3}] elongated along [010] was used to collect Laue data on station 9.5 (Brammer, Helliwell, Lamb, Liljas, Moore, Thompson & Rathbone, 1988; Thompson, Habash, Harrop, Helliwell, Nave, Atkinson, Hasnain, Glover, Moore, Harris, Kinder & Buffey, 1992) at the synchrotron radiation source of the SRS at the Daresbury Laboratory. An image-plate system (Mar Research Scanner, diameter 180 mm) implemented at the station was used as the detector. The SRS operated at 2 GeV with a current of 195 mA and the wiggler at 5 T.

The illuminating white beam spectral range was $0.4 \leq \lambda \leq 2.0$ Å. The crystal-to-image-plate distance was 138 mm. 20 images were recorded at 10° intervals, each with an exposure time of 0.3 s and an overall duty cycle time of 2.5 min. The total collection time for all these images was less than 1 h. One example of a recorded image from the image plate is shown in Fig. 1(*a*) and the average spot profile of this data is shown in Fig. 1(*b*). The pixel size is 150 μm^2. It can be seen that the spots are circular with a FWHM of 350 μm (*i.e.* recorded over three square pixels). For comparison, Fig. 2(*a*) shows the Laue photograph for the same orientation of the crystal (crystal-to-film distance 60 mm). An average spot profile for this data is shown in Fig. 2(*b*). The pixel size is now 50 μm^2. The spot is now clearly seen to be sharply streaked with a FWHM of 120 μm

in width and 350 μm in length; the spot shape and size is determined here by the size of the sample and its mosaic spread, since film has a negligible point-spread factor.

3. Data analysis

Laue reflections were processed up to 0.95 Å resolution using the wavelength range 0.36–1.50 Å. The Daresbury Laboratory Laue software package (Helliwell, Habash, Cruickshank, Harding, Greenhough, Campbell, Clifton, Elder, Machin, Papiz & Zurek, 1989) modified for image-
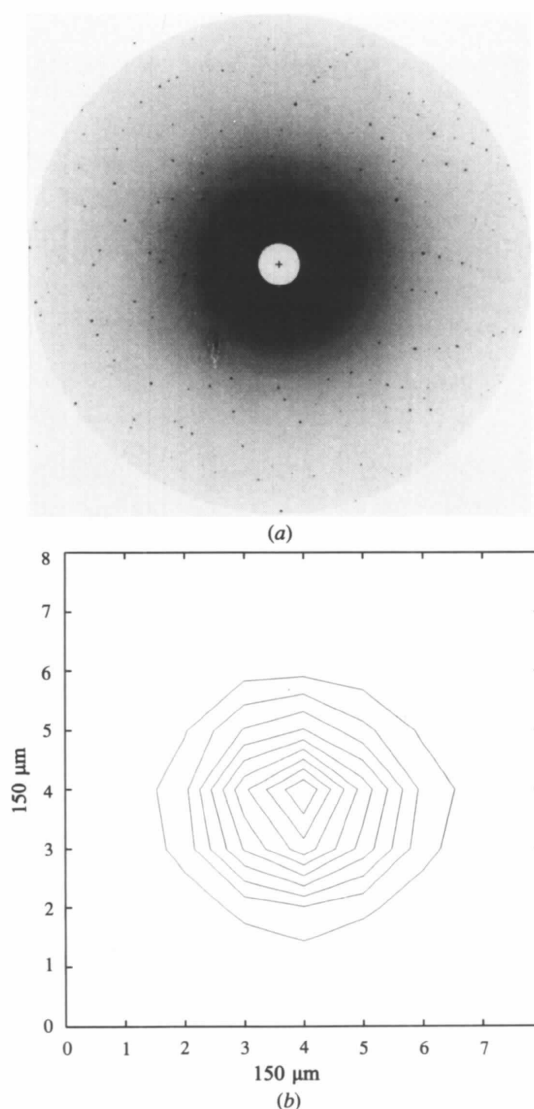

(*a*)

(*b*)

Figure 1
(*a*) Image-plate exposure from the NiAPO crystal. Crystal-to-plate distance 138 mm. The background is high due, in part, to the small crystal size, and also because the sample contains nickel; there is, of course, scope for improving the collimation and background control for such a sample. (*b*) Contour plot for the intensity of an average spot from the image in (*a*). The maximum value of 100 is arbitrarily chosen as the maximum intensity with contour intervals of 10. The pixel size is 150 μm.

plate data (J. W. Campbell, unpublished work) was used. There were no spatially overlapped spots. The unit-cell parameters and space group were available from the diffractometer study prior to data collection (Helliwell *et al.*, 1993). However, the unit-cell parameters were further refined (*i.e.* b and c, with a fixed) against the observed spot positions on each image. The r.m.s. deviation between observed and predicted spot positions was 0.031 (6) mm calculated over all the images. Table 1 compares the cell parameters for the three methods, Cu $K\alpha$, Mo $K\alpha$ and this Laue study.

LAUENORM was used for wavelength normalization. The wavelength range used was 0.455–1.180 Å and 6089 measured reflections were output. Fig. 3 shows the lambda
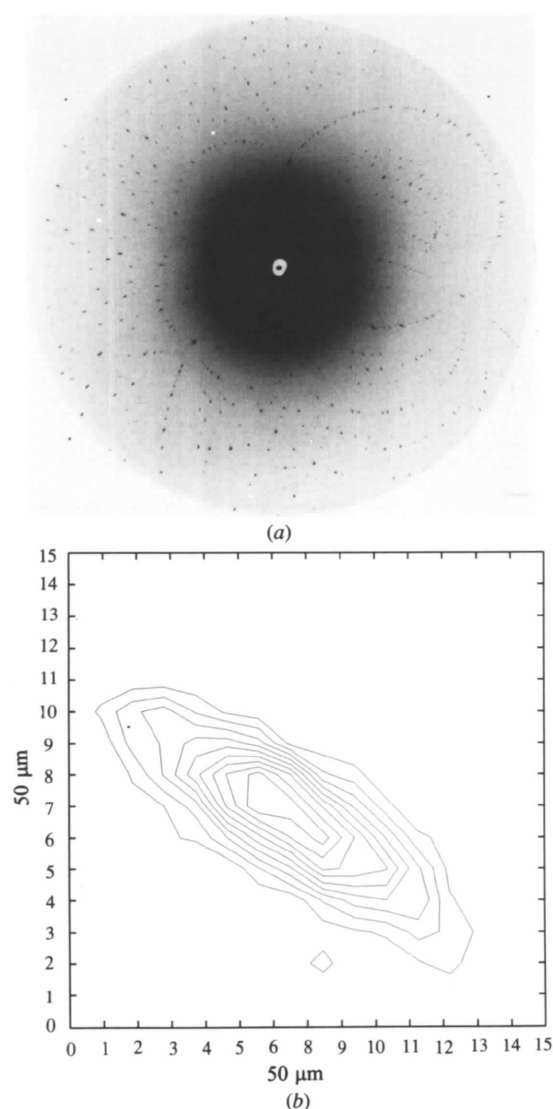
Table 1
Cell parameters for the three data sets.

Data set	a (Å)	b (Å)	c (Å)	β (°)	V (Å³)
Cu $K\alpha$	10.0209 (8)	15.661 (1)	14.0914 (8)	101.216 (5)	2169.3
Mo $K\alpha$	10.03 (2)	15.67 (2)	14.14 (2)	101.3 (1)	2180
Laue*	10.02	15.728 (6)	14.134 (6)	101.313 (14)	2184.16

*The refinement in *LAUEGEN* is displayed to two decimal places. The values given here are the averages over all 20 images and yield the values to three decimal places, and standard deviations, as shown. These average values have then been used for processing from *LAUEGEN* onwards. The a cell parameter was held fixed. As a test b and c were held fixed and a refined against five images. The value remained constant at 10.02 Å.

curve for this image-plate data set. A unique set of data was produced by the programs *ROTAVATA/AGROVATA* (Collaborative Computing Project No. 4, 1994). The merging R factor (on *I*) was 10.6% for 6048 measurements (41 reflections rejected), giving 1896 unique data. The completeness of the data for ∞–d_{min}, ∞–$2d_{min}$ and $2d_{min}$–d_{min} was 67.6, 55.7 and 68.8%, respectively. The Ni-atom position was determined from the Patterson map using *SHELXS*86 (Sheldrick, 1985). The remaining atom positions were located by difference Fourier cycling.

With *SHELXL*93 (Sheldrick, 1992) and singlet data it is possible to make allowance for the f' and f'' variation with wavelength using the values of f' and f'' of Sasaki (1989). This was not necessary in this case because the variation for Ni in the wavelength range used is very small. Instead, the average value for Ni in this wavelength range was input.
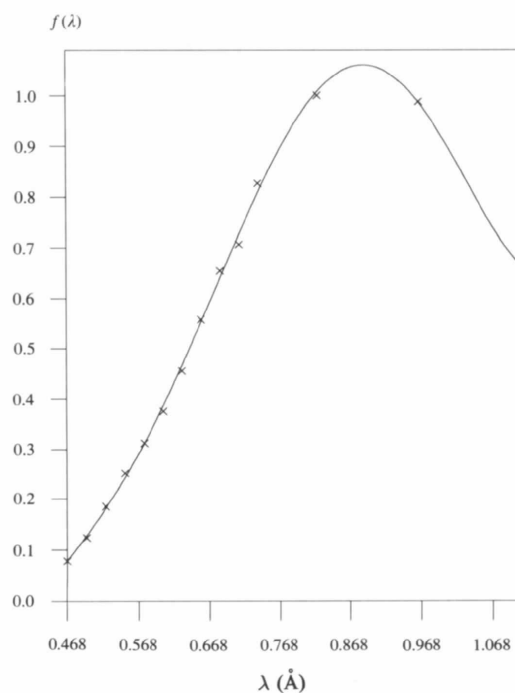

(a)

(b)

Figure 2
(a) Photographic film exposure from NiAPO. The same crystal is in the same orientation as used for the exposure in Fig. 1(a). Crystal-to-film distance 60 mm. (b) Contour plot for the intensity of an average spot from the photographic film exposure in (a). The maximum value of 100 is arbitrarily chosen as the maximum intensity with contour intervals of 10. The pixel size is 50 μm.

Figure 3
Lambda curve for the image-plate data set determined using *LAUENORM*. The wavelength values plotted on the abscissa are averages for each wavelength bin.

For the singlet data, the refinement (excluding H atoms) converged at an anisotropic R factor (on F) of 8.81% using all data.

In the refinement of the full structure (still excluding H atoms), the atomic displacement parameters of the atoms were low with a minority even being negative. An absorption correction procedure (Maginn, Harding & Campbell, 1993) was then applied to try to alleviate the problem. *SHELXL*93 produced a set of h, k, l and F_{calc} values from the best isotropic refinement. *LAUESCALE* used the F_{calc} values to apply an absorption surface to each original image. The absorption surface produced for the image in Fig. 1(a) is shown in Fig. 4. A new absorption-corrected final set of h, k, l, F, $\sigma(F)$ and λ values was then produced. The merging factor (on I) for *LAUESCALE*, now with 6472 singlet measurements (greater than *LAUENORM*'s 6089 measurements due to a slightly different acceptance procedure), was 10.9% producing 1979 unique measurements. The completeness of the data for $\infty-d_{min}$, $\infty-2d_{min}$ and $2d_{min}-d_{min}$ was 70.6, 56.5 and 72.0%, respectively.

The final set of absorption-corrected data was then used with *SHELXL*93 and the structure refined again isotropically. All H atoms connected to the C and N atoms in the structure were then generated in their calculated positions. All atoms, with the exception of H atoms, were then refined anisotropically (310 parameters) with the refinement converging to a final R (on F) of 7.90% for 1934 unique measurements accepted by *SHELXL*93, 5.11% for $I > 3\sigma(I)$ (1397 measurements). Sensible values were then achieved for the atomic displacement parameters.*

---

* Lists of structure factors, anisotropic thermal parameters and the principal interatomic distances and angles have been deposited with the IUCr (Reference: HI0010). Copies may be obtained through The Managing Editor, International Union of Crystallography, 5 Abbey Square, Chester CH1 2HU, England.
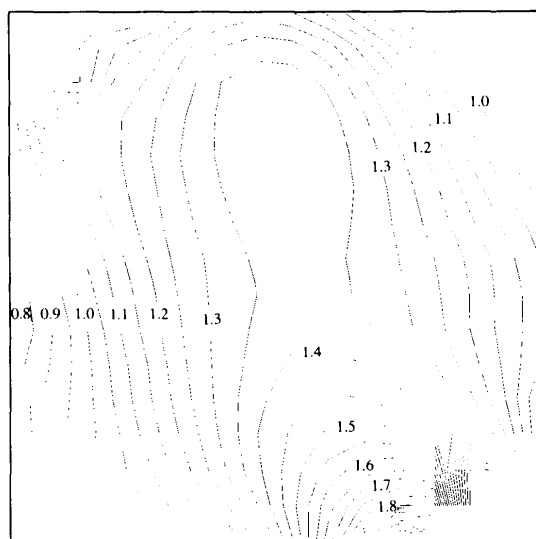

Figure 4
Absorption surface contour plot produced by *LAUESCALE* for the image-plate exposure shown in Fig. 1(a).

Table 2
Atomic coordinates ($\times 10^4$) and B_{eq} values for NiAPO derived from synchrotron Laue IP data.

Atom	x	y	z	$B_{eq}\dagger$ (Å^2)
Ni1	-8833 (1)	7711 (1)	1354 (1)	0.87 (4)
P1	-5496 (2)	7930 (1)	1425 (2)	0.61 (4)
P2	-23 (2)	7855 (1)	3402 (2)	0.61 (4)
P3	-2301 (2)	9938 (1)	4382 (2)	0.68 (4)
P4	-2725 (2)	9833 (1)	737 (2)	0.68 (4)
Al1	-2767 (2)	8781 (1)	2570 (2)	0.61 (4)
Al2	-5027 (2)	6233 (1)	365 (2)	0.61 (4)
Al3	-5010 (2)	8846 (1)	-491 (2)	0.65 (4)
O1	-6766 (5)	7998 (3)	1802 (4)	0.99 (8)
O2	-9169 (6)	8088 (3)	2700 (4)	0.91 (8)
O3	-9160 (6)	9028 (3)	1034 (4)	1.37 (8)
O4	-4291 (6)	8276 (3)	2154 (4)	1.06 (8)
O5	-5164 (6)	7000 (3)	1227 (4)	1.06 (8)
O6	-5596 (5)	8401 (3)	463 (4)	0.95 (8)
O7	-1535 (6)	8035 (3)	3053 (4)	0.99 (8)
O8	-3034 (5)	9517 (3)	3446 (4)	0.87 (8)
O9	-2201 (5)	9235 (3)	1593 (4)	1.14 (8)
O10	-4535 (5)	6664 (3)	-641 (4)	0.87 (4)
O11	-3887 (6)	5453 (3)	878 (4)	0.98 (8)
O12	-6655 (6)	5792 (3)	56 (4)	0.95 (4)
O13	-3203 (6)	10451 (3)	4846 (4)	1.14 (8)
O14	-6133 (6)	9628 (3)	-1012 (3)	1.14 (8)
O15	-4899 (6)	8102 (3)	-1377 (4)	0.95 (8)
O16	-3386 (6)	9276 (3)	-120 (4)	1.18 (8)
O17	-1574 (6)	10327 (4)	524 (4)	1.40 (8)
O18	-5322 (8)	5803 (5)	2836 (6)	2.77 (8)
N1	-8637 (9)	7483 (5)	-68 (7)	1.52 (8)
N2	-10906 (9)	7453 (4)	809 (7)	1.48 (8)
N3	-8238 (7)	6482 (4)	1874 (6)	1.40 (8)
N4	-7439 (8)	4601 (4)	1893 (6)	1.56 (8)
C1	-9953 (11)	7181 (8)	-629 (9)	2.20 (11)
C2	-11109 (12)	7557 (7)	-288 (10)	2.16 (15)
C3	-9128 (9)	5739 (5)	1791 (7)	1.41 (11)
C4	-8558 (11)	4959 (5)	2302 (8)	1.63 (11)

$\dagger B_{eq} = (8\pi^2/3)\sum_i\sum_j U_{ij}a_i^*a_j^*\mathbf{a}_i.\mathbf{a}_j$.

All diagrams were produced using *TEXSAN* software (Molecular Structure Corporation, 1985). The atomic positional parameters are listed in Table 2, in a similar format to the table presented for the Cu $K\alpha$ and Mo $K\alpha$ results of Helliwell *et al.* (1993) to facilitate comparison.

4. Discussion

The refined structure obtained agrees well with that derived from earlier monochromatic studies (Helliwell *et al.*, 1993). The final R factors and data-to-parameter ratios for the Laue, Cu $K\alpha$ and Mo $K\alpha$ are 7.9%, 6.2; 5.7%, 11.32; 5.0%, 5.97, respectively. Fig. 5 shows one molecule of the structure. To illustrate the quality of the structure, the actual values of some of the bond distances from this study will now be given with the estimate from the earlier monochromatic Cu $K\alpha$ study given in square brackets. The average Ni—O bond distance is 2.102 (21) [2.097 (12) Å] and Ni—N bond distance is 2.103 (11) [2.111 (7) Å]. Two types of P—O bond distances exist: P—O linked to Al and P—O linked to Ni. Their average distances are 1.537 (7) [1.542 (9)] and 1.478 (1) [1.482 (1) Å], respectively. Further details of the structure and its chemistry can be found in

Rajic, Stojakovic & Kaucic (1991) and Helliwell *et al.* (1993) and references therein.

The refined structures from the Laue data and monochromatic data were overlapped with one another by a least-squares determination of a rotation matrix and a translation vector. This provides an overall idea of the structural accuracy. The r.m.s. deviation (Å) and maximum single atomic displacement (in parentheses) for the Laue:Cu $K\alpha$, Laue:Mo $K\alpha$ and Cu $K\alpha$:Mo $K\alpha$ cases (all atoms except H) were 0.030 (0.074), 0.034 (0.095) and 0.027 (0.060), respectively. The thermal parameters can be compared by taking the ratio $B_{Laue}/B_{Cu\,K\alpha}$, which has the value 0.64. This can be compared with the value $B_{Mo\,K\alpha}:B_{Cu\,K\alpha}$ of 0.86 (Helliwell *et al.*, 1993).

We can conclude that a good quality refinement has been realized for this structure using a small crystal. In particular, the use of the on-line image-plate device proved to be very effective for the synchrotron Laue data collection for this small crystal with data collection taking less than 1 h.
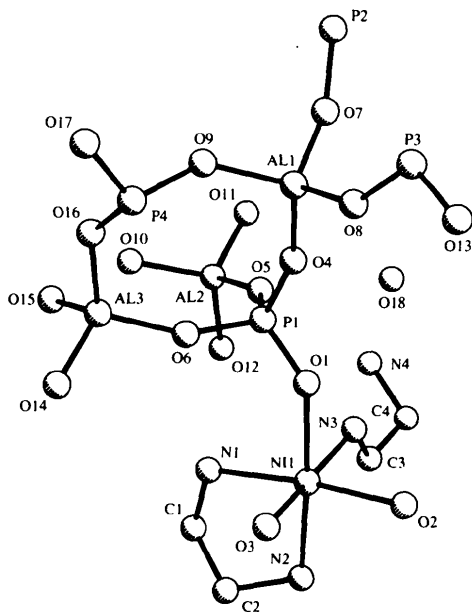
Figure 5
The asymmetric unit of NiAPO, with H atoms omitted.

References

Allinson, N. M. (1993). *Synchrotron Rad. News*, **6**, 4–6.
Allinson, N. M. (1994). *J. Synchrotron Rad.* **1**, 54–62.
Andrews, S. J., Papiz, M. Z., McMeeking, R., Blake, A. J., Lowe, B. M., Franklin, K. R., Helliwell, J. R. & Harding, M. M. (1988). *Acta Cryst.* **B44**, 73–77.
Bilderback, D. H., Thiel, D. J., Pahl, R. & Brister, K. E. (1994). *J. Synchrotron Rad.* **1**, 37–42.
Brammer, R., Helliwell, J. R., Lamb, W., Liljas, A., Moore, P. R., Thompson, A. W. & Rathbone, K. (1988). *Nucl. Instrum. Methods*, **A271**, 678–687.
Collaborative Computing Project No. 4 (1994). *Acta Cryst.* **D50**, 760–763.
Clucas, J. A., Harding, M. M. & Maginn, S. J. (1988). *J. Chem. Soc. Chem. Commun.* pp. 185–187.
Coppens, P. (1992). *Synchrotron Radiation Crystallography*. New York: Academic Press.
Euler, H., Gilles, R. & Will, G. (1994). *J. Appl. Cryst.* **27**, 190–192.
Harding, M. M. (1990). *Chem. Br.* pp. 956–958.
Harding, M. M. (1991). *J. Phys. Chem. Solids*, **10**, 1293–1298.
Helliwell, J. R., Habash, J., Cruickshank, D. W. J., Harding, M. M., Greenhough, T. J., Campbell, J. W., Clifton, I. J., Elder, M., Machin, P. A., Papiz, M. Z. & Zurek, S. (1989). *J. Appl. Cryst.* **22**, 483–497.
Helliwell, M., Gallois, B., Kariuki, B. M., Kaucic, V. & Helliwell, J. R. (1993). *Acta Cryst.* **B49**, 420–428.
Helliwell, M., Gomez de Anderez, D., Habash, J., Helliwell, J. R & Vernon, J. (1989). *Acta Cryst.* **B45**, 591–596.
Maginn, S. J., Harding, M. M. & Campbell, J. W. (1993). *Acta Cryst.* **B49**, 520–524.
Molecular Structure Corporation (1985). *TEXSAN. TEXRAY Structure Analysis Package*. MSC, 3200 Research Forest Drive, The Woodlands, TX 77381, USA.
Rajic, N., Stojakovic, D. & Kaucic, V. (1991). *Zeolites*, **11**, 612–616.
Riekel, C. (1993). *ESRF Beamline Handbook*, pp. 53–56. ESRF, Grenoble, France.
Sasaki, S. (1989). KEK/Photon Factory Report 88–14. National Laboratory for High Energy Physics, Tsukuba, Japan.
Sheldrick, G. M. (1985). *SHELXS86. Program for the Solution of Crystal Structures*. Univ. of Göttingen, Germany.
Sheldrick, G. M. (1992) *SHELXL93. Program for Crystal Structure Refinement*. Univ. of Göttingen, Germany.
Thompson, A. W., Habash, J., Harrop, S., Helliwell, J. R., Nave, C., Atkinson, P., Hasnain, S. S., Glover, I. D., Moore, P. R., Harris, N., Kinder, S. & Buffey, S. (1992). *Rev. Sci. Instrum.* **63**(1), 1062–1064.
Wilkinson, C. (1994). *Biophys. Chem.* In the press.